Incomplete fusion reactions in $^{16}O + ^{165}Ho$

ANIL SHARMA[1], B BINDU KUMAR[1], S MUKHERJEE[1*], S CHAKRABARTY[2],
B S TOMAR[2], A GOSWAMI[2], G K GUBBI[2], S B MANOHAR[2], A K SINHA[3]
and S K DATTA[3]

[1] School of Studies in Physics, Vikram University, Ujjain 456 010, India
[2] Radiochemistry Division, Bhabha Atomic Research Centre, Mumbai 400 085, India
[3] Nuclear Science Centre, Aruna Asaf Ali Marg, New Delhi 110 067, India
*Address for correspondence: B-4/4, Teachers' Quarters, Vikram University Campus, Kothi Road,
Ujjain 456 010, India

Abstract. Excitation functions for evaporation residues of the system $^{16}O + ^{165}Ho$ have been measured up to 100 MeV. Recoil range distribution of long lived reaction products were measured at ^{16}O beam energy of 100 MeV. Detailed Monte Carlo simulation of recoil range distributions of products were performed with the help of PACE2 code, in order to extract the contributions of incomplete fusion in the individual channels. The results clearly show the incomplete fusion contributions in the tantalum and thulium products. This is confirmed by the predictions of breakup fusion model of the incomplete fusion.

Keywords. Heavy ion reactions; incomplete fusion; recoil range distribution; activation technique; Monte Carlo simulation.

PACS Nos 25.70.Gh; 25.70.Jj

1. Introduction

It is now generally recognized that several reaction mechanisms are operative in heavy-ion-induced reactions below 10 MeV/amu. Predominant among these are, complete fusion (CF), deep-inelastic collision (DIC), and quasi-elastic collisions. As the projectile energy increases to 5–10 MeV/amu and above, it turns out that the fused system does not consist of the sum total of all the nucleons involved. There are particles which can be emitted from either of the heavy ions before they fuse. In the laboratory system these particles are either very fast (much faster than those coming from an evaporation process) if they are emitted by the projectile or possibly very slow if they are emitted from the target. The fast particles are forward peaked. They consist of nucleons as well as clusters of nucleons like alpha particle. Such a process, where the remaining part of the projectile and of the target fused together after the initial colliding nuclei have emitted light particles, has been called incomplete fusion (ICF), breakup fusion or massive transfer.

These reactions were first observed by Kaufmann and Wolfgang [1] in 100 MeV ^{16}O induced reactions on ^{103}Rh. Subsequently Britt and Quinton [2] observed forward peaked alpha particles having velocity close to the incident beam. The most unambiguous evidence for incomplete fusion was observed by Inamura *et al* [3] by measurement of forward peaked alpha particles in coincidence with prompt gamma rays of the heavy residues formed in ^{14}N + ^{159}Tb reactions. Earlier studies of ICF were centered around beam energies above 10 MeV/amu. Alexander and Winsberg [4] were the first to comment on partial momentum transfer in the ICF process, wherein the incompletely fused composite nucleus does not show total linear momentum of projectile and target. Hence, the measurement of the linear momentum will give an insight into the reaction mechanism. The topic of incomplete fusion was reviewed by Gerschel [5], Siemssen [6] and Ngo [7] in early eighties. Several models are used to explain these ICF namely, sum rule model [8], breakup fusion model [9], promptly emitted particles (PEPs) model [10], exciton model [11], etc. During the past decade a large number of reports have appeared [12–14] showing the occurrence of incomplete fusion at beam energy just above the Coulomb barrier.

Recoil range distribution (RRD) measurements are particularly attractive for studying these ICF reactions. When a single reaction product is formed via several reaction routes, the linear momentum transfer contains the signature of their mechanism. Parker *et al* [15] have shown that a differential recoil range distribution may be decomposed to evaluate the extent of the variety of mechanisms. Recently, this method has been used in studies of complete and incomplete fusion at energies $\sim$5–10 MeV/amu. These include ^{12}C on ^{197}Au [16], ^{12}C on ^{93}Nb and ^{16}O on ^{89}Y [12], ^{12}C on ^{89}Y and ^{103}Rh [13,14]. These data were analysed for various CF and ICF processes. For ^{16}O there are four dominant processes: complete fusion, ^{12}C, ^{8}Be and α transfer. However, in the heavy systems, such as ^{16}O on ^{165}Ho used in the present work, the charged particle emission from compound nucleus (CN) is hindered because of the high Coulomb barrier. For such system the only important de-excitation mode for the CN and excited intermediate nuclei is through neutron evaporation, so that each final product is formed essentially through a single route. It is therefore interesting to study the reaction products, such as, tantalum and thulium products, which cannot be formed via complete fusion of ^{16}O with ^{165}Ho and subsequent de-excitation by alpha and nucleon evaporation in the usual way.

The objective of the present work, therefore, is to study the complete and incomplete fusion of ^{16}O with ^{165}Ho up to 100 MeV. Incomplete fusion processes at these energies are by no means negligible, even for heavy targets like holmium with substantial Coulomb barriers. Earlier Parker *et al* [16] in their study of complete and incomplete fusion of ^{12}C with ^{197}Au have found that incomplete fusion events represent about 20% of the reaction cross section, including more than half of all non-fission events. In the present work, the experiment includes the measurement of recoil range distribution of a number of radioactive isotopes. Finally, the experimental results were compared with Monte Carlo simulation code PACE2 for the complete fusion part of the reaction and the incomplete fusion part is deduced by extracting the complete fusion part from the experimental data followed by the comparison with the predictions of the breakup fusion model.

2. Experimental procedure

Experiments for the measurement of excitation functions were carried out at Nuclear Science Centre (NSC) pelletron facility, New Delhi and BARC–TIFR pelletron accelerator at

Mumbai, India. Stacks of three self supported (about 600 μg/cm^2) holmium metal target foils interspersed with 2 mg/cm^2 thick Al foils were irradiated with ^{16}O beam. Irradiation time of about 1–2 hours was selected according to the half-lives of the radioisotopes produced. The radionuclides produced in each target catcher assembly were then identified by counting the foils successively on a pre-calibrated 60cc HPGe detector coupled to a 4K MCA. The efficiency of the detector as a function of gamma ray has been determined using standard ^{152}Eu source. The detector resolution was 2 keV at 1332 keV. Each foil was counted for 300 seconds duration immediately after activation. Subsequently, the foils were recounted for successively longer duration over a period of two weeks. The total count rates in any counting was kept less than 10,000 counts per sec to reduce dead time losses. The yields of the radionuclides identified in each foil were determined using the published half-lives, and branching ratios [17]. Table 1 lists the nuclear spectroscopic data for the nuclides for which the excitation functions were measured in the work. The spectra were analysed using PC version of the SAMPO program. The cross sections for a particular product in different foils were obtained using the equation reported elsewhere [13].

Recoil range distribution for a number of radioactive products of the reaction ^{16}O + ^{165}Ho caught in a stream of aluminium foils were measured at ^{16}O beam energy of 100 MeV. The targets used were metallic holmium of thickness around 100 μg/cm^2 vacuum evaporated onto thin (100 μg/cm^2) aluminium backing. The catchers used were evaporated aluminium foils, typically 100 μg/cm^2 thick. After the irradiation, the activities of individual reaction products were measured by following the gamma ray activities of the evaporation residues (ERs) in individual catcher foils for a period of two weeks. The cross section (σ) for a particular reaction product in different foils were obtained using the equation reported earlier [13]. The yield distribution as a function of depth in the catcher stack was obtained for each product by dividing the yield in each catcher by its measured thickness and plotting the resulting activity density against cumulative catcher thickness to obtain the RRD. The accuracy of these distributions was limited by the uncertainty in determining the catcher thickness, generally about 5%. The RRDs were normalized using the cross section obtained in the excitation function measurement discussed above.

Table 1. Decay characteristics of the residual nuclei in ^{16}O + ^{165}Ho reactions.

ERs	Spin	Half-life	E_γ (keV)	I_γ(%)
^{178}Re	3^+	13.2 m	237	45
^{177}Re	$5/2^-$	14 m	197	8.4
^{176}Re	3^+	5.2 m	240	48
^{177}W	$1/2^-$	2.25 h	186.3	16.1
^{176}W	0^+	2.3 h	100.2	73.01
^{175}Ta	$7/2^+$	10.5 h	349	11.4
^{174}Ta	3^+	62.6 m	206.5	57
^{173}Ta	$5/2^-$	3.56 h	172.2	17.5
^{166}Tm	2^+	7.7 h	778.8	18.1

3. Analysis of experimental data

The excitation function measured for the radionuclides produced in the reaction ^{16}O + ^{165}Ho are shown in figures 1–3. The solid lines are eye guides to the experimental points.
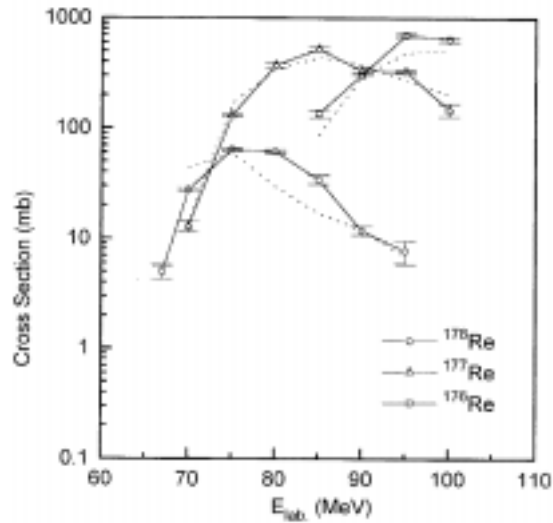

Figure 1. Excitation functions of evaporation residues $^{176-178}$Re in ^{16}O+ ^{165}Ho reaction. The solid lines are an eye guide to the experimental data. The dashed lines represent the PACE2 predictions for CF formations of ERs.
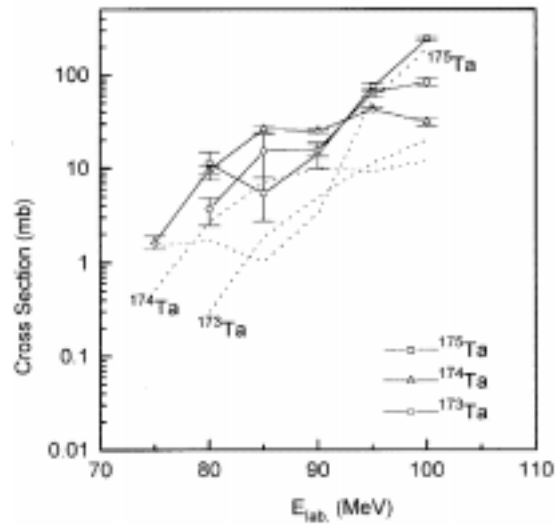

Figure 2. Excitation functions of evaporation residues $^{173-175}$Ta in ^{16}O+ ^{165}Ho reaction. Rest is same as in figure 1.
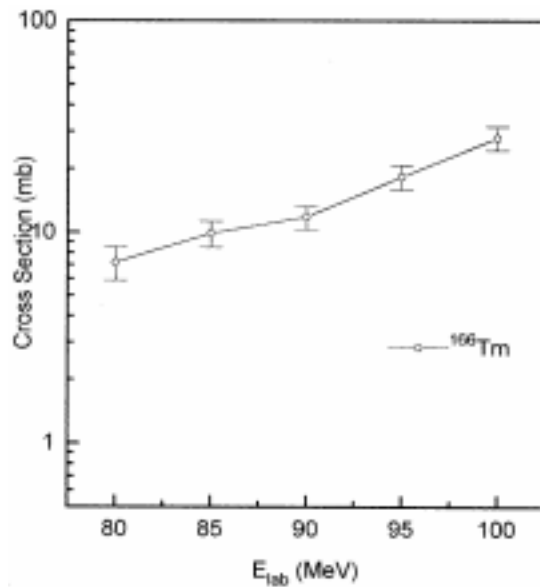
Figure 3. Excitation functions of evaporation residues ^{166}Tm in ^{16}O+ ^{165}Ho reaction. Rest is same as in figure 1.

The errors on the cross section arise mostly from the counting statistics (1–4%), target thickness (5–8%), detection efficiency (4%), beam fluence ($<$5%) and gamma-ray intensity values (5–10%). The dashed curves show the predictions obtained from the Monte Carlo simulation code PACE2 with level density parameter a taken as $A/7$ MeV^{-1}. The optical model parameters for alphas, protons and neutrons were taken from Perey and Perey [18]. The average gamma transition strengths used were from Endt [19]. The spin cut-off factor was taken to be 0.7 times the rigid body value, and using excited states of six nuclides to generate level density at lower excitation energy (E^*). For lower beam energies (67, 70 and 75 MeV) the BASS formula gave lower values of fusion cross section (σ_{fus}). Hence coupled channel code (CCFUS) [20] was used to calculate σ_{fus} by supplying ground state deformation of projectile and target as input, and inelastic channel coupling was taken into account. Default values were used for the other input parameters.

Figure 4 shows the differential recoil range distribution for the various reaction products studied in the present work at 100 MeV beam energy. The solid lines are eye guides to the experimental points. The cross section in each foil was plotted against the projected range along the beam axis. The PACE2 code gives the double differential cross section ($\text{d}^2\sigma/\text{d}E\text{d}\Omega$) for ERs, which is transformed into the projected range distribution along the beam axis. The predicted RRDs are shown as dashed curves. The ICF component was obtained by subtracting the CF component from the experimental curves and is shown as the dash-dotted curves. The simulation of the ICF process based on the breakup fusion model are represented by the dotted curves.
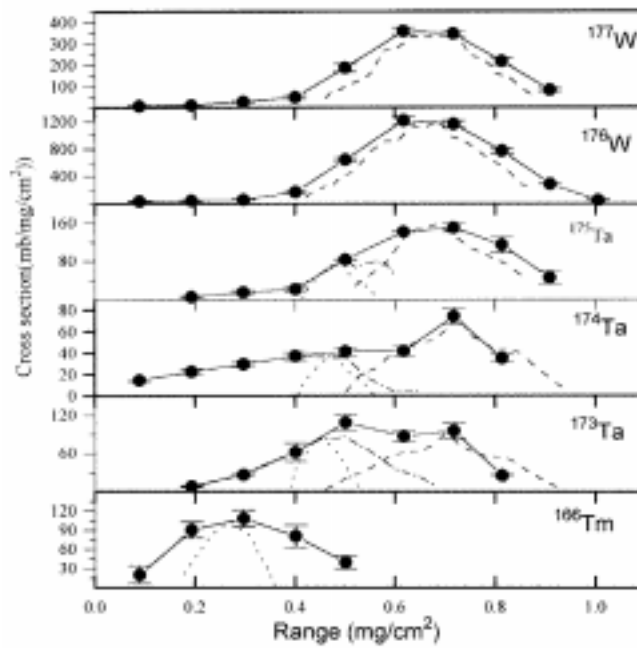
Figure 4. RRDs of evaporation residues in ^{16}O+ ^{165}Ho reaction at 100 MeV. The continuous lines are an eye guide to the experimental data. Dashed lines are the PACE2 predictions for CF formation of ERs. The dashed-dotted lines represent the ICF component obtained by subtracting the PACE2 predictions from the experimental data. Dotted lines are the simulated RRDs for ICF based on break-up fusion model.

4. Discussion

It can be seen from figure 1 that the excitation functions for the neutron emission products i.e. $^{176-177}$Re are well reproduced by the PACE2 calculations. However, for the product ^{178}Re there is a disagreement between theory and experiment, in the energy region 75 to 85 MeV. This disagreement is due to a finite Monte Carlo sample used in the calculated cross section. It was observed that this finite sampling in the calculations introduce an error of 25%, 10% and 1% for $\sigma = 1$ mb, 10 mb and 100 mb respectively. Within the limitations of the present theoretical calculations it can be remarked that these products are formed mainly via complete fusion of the projectile ^{16}O with the target nucleus ^{165}Ho.

Figures 2 and 3 show the excitation functions for $^{173-175}$Ta and ^{166}Tm products, respectively. It can be seen that for both $^{173-175}$Ta and ^{166}Tm products the experimentally measured cross sections are higher than those calculated with PACE2 code. From the above observations it can be inferred that in the case of ^{16}O + ^{165}Ho reactions the projectile ^{16}O breaks into α and ^{12}C followed by fusion of either of the two with the target nucleus ^{165}Ho, to give ^{166}Tm and $^{173-175}$Ta products, respectively. This is evidenced by the higher cross-sections for ^{166}Tm and $^{173-175}$Ta isotopes. The enhanced cross-sections

for the above products can be attributed to ICF. Wilczynski *et al* [8] explained the ICF in terms of sum-rule model. Similarly Udagawa *et al* [9] also proposed breakup fusion model in order to explain the outgoing particle spectra. However, these ICF reactions were studied at beam energy above 10 MeV/amu whereas in the present work ICF has been observed at projectile energies as low as 6 MeV/amu. Similar results were earlier obtained by Parker *et al* [15], Tomar *et al* [12], Bindu Kumar *et al* [13,14]. The above observations regarding the existence of ICF in the present energy range, can be confirmed by the study of linear momentum transfer with the measurement of recoil range distributions as discussed below.

Figure 4 shows the RRD of various reaction products studied in the present work at 100 MeV. In the present work $^{176-177}$W isotopes observed are produced in the ^{16}O + ^{165}Ho reaction through decay of higher Z precursors, namely $^{176-177}$Re with considerably short half-lives. We have only measured the cumulative cross sections of $^{176-177}$W, which have considerably longer half-lives than their precursors.

The cumulative cross sections were measured only after the complete decay of $^{176-177}$Re products to the respective $^{176-177}$W products. Thus in the measured cross sections of $^{176-177}$W the independent production cross section of $^{176-177}$Re is the dominant contribution. Similarly the RRDs of $^{176-177}$W essentially represent those of $^{176-177}$Re. The simulated RRDs for $^{176-177}$W and ^{175}Ta were corrected for the straggling due to stopping of the recoil products in the catcher foils, and finite target thickness using the formalism given by Winsberg and Alexander [21]. Figure 4 shows the experimental and theoretical RRDs. It is seen that the experimental RRDs for $^{176-177}$W agree with the calculated results. This shows that the rhenium products are mainly produced following the complete fusion of ^{16}O with ^{165}Ho. The RRDs for tantalum products (α, xn channels) deviate from the prediction of PACE2 code in all the three cases, namely, $^{173-175}$Ta. In the above cases the experimental curves show a low range component and a shoulder on the higher range side. This additional component in the low range side corresponds to the ICF process ^{165}Ho (^{16}O, α) ^{177}Ta*. This is indicated by the simulated RRD for ICF based on the breakup fusion model as shown in the figure by dotted lines. The ICF components in the RRD were obtained by subtracting the CF component from the experimental curve and is shown as dash-dotted in the respective figures. The RRD for ^{166}Tm in the ^{16}O+^{165}Ho system shows only the ICF component as indicated by the dotted curve obtained as simulated RRD for ICF based on breakup fusion model, corresponding to the ICF process ^{165}Ho(^{16}O, ^{12}C) ^{169}Tm*.

From the above observations it can be inferred that there is a veritable signature of ICF process in the production of tantalum and thulium isotopes by the breakup of ^{16}O into ^{12}C and α with either of them fusing with target to give the respective products. In these reactions, α and ^{12}C act essentially as spectators during the formation of tantalum and thulium products. The linear momentum transfer to the target is reduced to 3/4 and 1/4 of compound nucleus value respectively. Table 2 indicates the contribution of CF and ICF cross sections in the yields of tantalum and thulium isotopes. Thus the present study indicates significant ICF contributions to the total reaction cross section even at as low energy as 6 MeV/amu in the case of light-heavy ion induced reactions. The study indicates that ICF contributions results from the breakup of projectile into two fragments ^{12}C+ α with either of the two fusing with the target thereby bringing in linear momentum transfer in the ratio of its mass to that of projectile.

Table 2. CF and ICF contributions in RRD of ^{16}O+ ^{165}Ho reaction (in mb).

Nuclei	CF	ICF (experimental)	ICF (simulated)
^{177}W	63.69±5.67	–	–
^{176}W	233.78±19.8	–	–
^{175}Ta	22.8±2.05	13.67±1.23	6.96±0.71
^{174}Ta	17.47±1.57	13.94±1.24	3.32±0.74
^{173}Ta	22.24±2.00	22.77±2.21	7.32±0.82
^{166}Tm	–	–	12.24±1.19

5. Conclusions

Excitation functions for radionuclides in the energy range 70–100 MeV were measured in ^{16}O + ^{165}Ho reaction. Recoil range distributions of evaporation residues of the same system at beam energy 100 MeV was also studied. Comparison with the prediction of Monte Carlo simulation code PACE2 shows enhancement in cross sections for the tantalum (^{174,173}Ta) and thulium(^{166}Tm) isotopes. The simulation of the RRDs confirm the occurrence of ICF in the formation of these evaporation residues. The incomplete fusion can be explained in terms of the breakup of ^{16}O projectile into ^{12}C and α followed by the subsequent fusion of either of the two parts.

Acknowledgements

References

[1] R Kaufmann and R Wolfgang, *Phys. Rev.* **121**, 192 (1961)
[2] H C Brit and A R Quinton, *Phys. Rev.* **C124**, 877 (1961)
[3] T Inamura, M Ishihara, T Fakuda, T Shimoda and H Hiruta, *Phys. Lett.* **B68**, 51 (1977)
[4] J M Alexander and L Winsberg, *Phys. Rev.* **121**, 529 (1961)
[5] C Gerschel, *Nucl. Phys.* **A387**, 297c (1982)
[6] R H Siemssen, *Nucl. Phys.* **A400**, 245c (1983)
[7] Ch Ngo, *Prog. Nucl. Part. Phys.* **16**, 139 (1985)
[8] J Wilczynski, K Siwek-Wilczynska, J VanDriel, S Gonggrijp, D C J M Hageman, R V F Janssens, J Lukasiak, R H Siemssen and S Y Van der Werf, *Nucl. Phys.* **A373**, 109 (1982)
[9] Udagawa and T Tamura, *Phys. Rev. Lett.* **45**, 1311 (1980)

[10] J P Bondroff, J N De, G Fai, A O T Karvinen and J Randrup, *Nucl. Phys.* **A333**, 285 (1980)

[11] M Blann, *Phys. Rev.* **C31**, 1285 (1985)

[12] B S Tomar, A Goswami, A V R Reddy, S K Das, P P Burte, S B Manohar and Bency John, *Phys. Rev.* **C49**, 941 (1994)

[13] B Bindu Kumar, S Mukherjee, S Chakrabarty, B S Tomar, A Goswami and S B Manohar, *Phys. Rev.* **C57**, 743 (1998)

[14] B Bindu Kumar, Anil Sharma, S Mukherjee, S Chakrabarty, P K Pujari, B S Tomar, A Goswami, S B Manohar and S K Datta, *Phys. Rev.* **C59**, 2923 (1999)

[15] D J Parker, J Asher, T W Conlon and N Naquib, *Phys. Rev.* **C30**, 143 (1984)

[16] D J Parker, P Vergani, E Gadioli, J J Hogan, F Vettore, E Gadioli-Erba, E Fabrici and M Galmarini, *Phys. Rev.* **44**, 1528 (1991)

[17] U Reus and W Westmeier, *At. Data Nucl. Data Tables* **29**, 1 (1983)

[18] C M Perey and F G Perey, *At. Data Nucl. Data Tables* **17**, 1 (1976)

[19] P M Endt, *At. Data Nucl. Data Tables* **26**, 47 (1981)

[20] C H Dasso and S Landowne, *Comput. Phys. Commun.* **46**, 187 (1987)

[21] L Winsberg and J M Alexander, *Phys. Rev.* **121**, 518 (1961)